NUMERICAL SIMULATION OF DRAFT TUBE FLOW IN OFF-DESIGN CONDITIONS

FIDEL ARZOLA, MSc.
CORPOELEC – CVG EDELCA, Ciudad Guayana, Venezuela
farzola@edelca.com.ve

LUIS ROJAS-SOLORZANO, PhD
Universidad Simón Bolívar, Caracas, Venezuela
rrojas@usb.ve

ABSTRACT

Draft tube flow fields are simulated with 3D unsteady Reynolds averaged Navier-Stokes equations. The purpose of this study is the modeling, simulation and characterization of a complex three-dimensional unsteady flow inside a Francis turbine draft tube for two specific off-design conditions: A) Part load (0.88Q), frequently characterized by the occurrence of an unsteady rotating vortex rope linked to strong pressure fluctuations and, B) High load (1.21Q), where softer pressure surges taking place because the cavity volume at this condition has an axisymmetric shape. This work takes place after overhaul works on the actual turbine, which include new runner and wicket gates and modifications on stay vanes and other passageways; where power output, efficiency and stable operating range were increased. The computational domain consists of the draft tube alone. A relative poor mesh (430k nodes) and the k-ε turbulence model are implemented in order to get a quick, but clear explanation to understand how the flow in the existing draft tube responds in front of a new velocity distribution at runner outlet for off-design conditions. Numerical results are qualitative and quantitatively analyzed and compared with experimental data from model and prototype. The unsteady and complex nature of the flow field distribution inside the draft tube for both conditions is visualized.

KEY WORDS: draft tube, numerical simulation, vortex rope, pressure fluctuation

INTRODUCTION

Francis turbines usually present unsteady flow fluctuations at partial loads, due to strong helical cavitating vortex rotating like a swirling rope in the center of the draft tube cone. The precession of vortex rope causes pressure fluctuations and vibrations which sometimes can lead to variations in the power output or/and shaft torque. On the other hand, Francis turbines experience the appearance of another cavitating vortex structure at high loads, typically called draft tube void, which is quite axisymmetric along the draft tube and generates lower pressure fluctuations; even though hydrodynamic gradients are small, there is a major susceptibility to the excitation of other frequencies in the hydroelectric unit and penstock due to natural frequencies of this cavitating structure. These self-excited instabilities appear because of the flow angle is not orthogonal at the runner outlet and also these are produced for a relative sudden variation in the cross section along the draft tube [1]. In the figure 1 a graphic description of both mentioned hydrodynamic phenomena is shown.

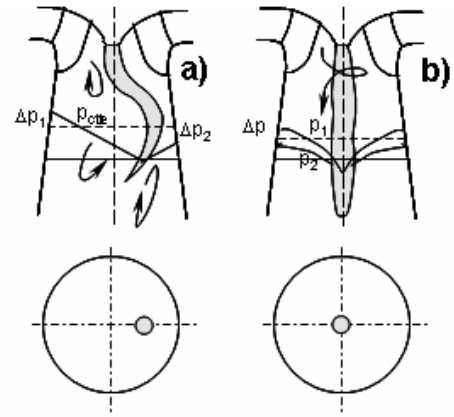

Figure 1: Off-design flow fields:
A) Vortex rope at partial loads, B) Draft tube void at high loads [1]

Greater complexity follows from the draft tube streamline curvature and the adverse pressure gradient caused by the diffusion due to the geometrical configuration and from the change of cross sectional shape. Each of these characteristics is known to be difficult to predict with numerical computations [2]. Many computational studies on the flow behavior inside hydraulic turbines and particularly, on the draft tube were presented in recent past years, being a lot of them with industrial application in order to get a greater stable operating range and to increase operational safety for the entire power plant.

The modern energy market dictates that the hydroelectric industry operates their hydraulic machines at off-design conditions due to rapidly changing user load conditions [2]. Off-design performance of hydraulic turbines is accompanied by strong fluctuating flow fields and hydrodynamic self-excited instabilities. Additionally, a large number of hydroelectric installations are ageing; this gives a rise to the potential for refurbishment to implementing changes in the design for improved efficiency and increase power output, as well as, greater stable operating range. Usually the runner and guide vanes are focused upon in the refurbishment process, but due to constructional costs and structural risks the spiral case and draft tubes are seldom redesigned. Unfavorable flow behavior occurs when the runner and draft tube are not properly matched; this causes an immediate reduction of the stable operating range of the machine. In fact, this case study, where ones of the largest Francis turbines were refurbished in Guri Power Plant in Venezuela, kept unaltered the existing draft tube design [3].

In this paper, the industrial motivation is to get a complete understanding of the flow behavior in an existing draft tube matched to a new hydraulic optimized runner. Both the computed pressure pulsations and static pressure recovery factor are compared with experimental measurements

showing good agreement. A qualitative study of the flow is presented for each operating condition by using primitive variable visualization. Even though it is well known that results are strongly affected by the damping of the turbulence model and for using steady and symmetrical boundary conditions, the vortex rope structure is well reproduced and its pressure pulsations have good correspondence with measurements in time and frequency domain. Nevertheless, at full load the axisymmetric void and its associated pressure pulsations were unsuccessfully simulated due to inability of the code to simulate the cavitation compliance; therefore, in this work it is reported velocity and pressure profiles distribution for this operating condition using a single phase model only.

NUMERICAL METHOD

All simulations were carried out with the 3D time-averaged Navier Stokes solver ANSYS CFX 10 which uses the Control-Volume Finite Element Method to solve governing equations for incompressible turbulent flow. For spatial discretisation, high resolution scheme is implemented for advection terms in order to achieve second order accuracy where possible and still obtaining sufficient numerical stability. For temporal discretisation, the 2nd-order Euler Backward scheme is applied, and furthermore, double precision is activated during code compilation in order to minimize mathematical round-off errors. For turbulence treatment the well-known two-equation model k-ε was implemented independent of wall distance. The simulations are transient with a time-step size equal to 0.01s or 6.75º runner rotation. All transient simulations are started from converged steady results. Governing equations for incompressible flow in vectorial form are as follow:

$$\nabla \bullet C = 0 \tag{1}$$

$$\frac{\partial C}{\partial t} + \nabla \bullet \left(C \times C \right) = \nabla p + \nabla \bullet \left(\mu_{eff} \nabla C \right) - \nabla \bullet \left(\mu_{eff} \nabla C \right)^T + S_M \tag{2}$$

Where $\boldsymbol{C}$ is the velocity vector, p is the local pressure, $\mu_{eff} = \mu + \mu_t$ is the effective viscosity accounting for turbulence effects and S_M is representing the source terms. The k-ε turbulence model introduces two new variables to the equations system modifying the equation (2) only, as follow:

$$\frac{\partial \rho C}{\partial t} + \nabla \bullet \left(\rho C \times C \right) = \nabla \bullet \left(\mu_{eff} \nabla C \right) + \nabla p' - \nabla \bullet \left(\mu_{eff} \nabla C \right)^T - B \tag{3}$$

Where B is the sum of body forces and p' is the modified pressure given by:

$$p' = p + \frac{2}{3} \rho k \tag{4}$$

The k-ε model assumes that the turbulence viscosity is linked to the turbulence kinetic energy and dissipation via the relation:

$$\mu_t = c_\mu \rho \frac{k^2}{\varepsilon} \tag{5}$$

This turbulence model solves transport equations for the turbulence kinetic energy (k) and the turbulence dissipation rate (ε) by means of following semi-empiric expressions:

$$\frac{\partial \left(\rho k \right)}{\partial t} + \nabla \bullet \left(\rho C k \right) = \nabla \bullet \left[\left(\mu + \frac{\mu_t}{\sigma_k} \right) \nabla k \right] + P_k - \rho \varepsilon \tag{6}$$

$$\frac{\partial(\rho\varepsilon)}{\partial t}+\nabla\bullet(\rho C\varepsilon)=\nabla\bullet\left[\left(\mu+\frac{\mu_t}{\sigma_\varepsilon}\right)\nabla\varepsilon\right]+\frac{\varepsilon}{k}(P_k c_{\varepsilon 1}-\rho\varepsilon c_{\varepsilon 2}) \quad (7)$$

Where P_k is the turbulence production due to viscous and buoyancy forces. $c_{\varepsilon 1}$, $c_{\varepsilon 2}$, σ_ε are constants.

DOMAIN AND COMPUTATIONAL GRID

A prototype scaled draft tube without runner geometry is used as domain with a 20 meters long attached volume at the outlet to permit a better flow development.

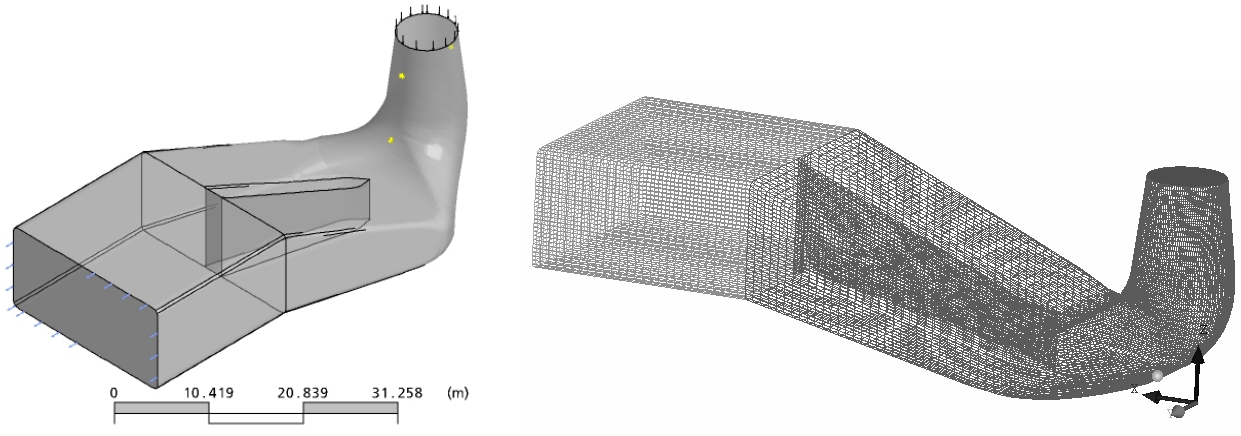

Figure 2: Computational domain and surface grid

With the rapid progress of computational performance, steady and unsteady numerical simulations have already become one of the important methods to study complex industrial flows, as for example,, rotating and unsteady flow in hydraulic turbines. At the present time, numerical simulation of flow fields inside elbow draft tubes has been studied by many researchers, most of them with enough powerful computational resources. This work is carried out with quite limited computing hardware; therefore, it was necessary to work with a mesh coarser than common ones (e.g., typically for draft tube alone, between 1.5 and 8 million nodes are common [4]). Structured hexahedral elements are generated using ANSYS ICEM-CFD, the cone and elbow have an O-grid mesh, with refinement in the volumetric center of the draft tube where cavitating structures take place. The final volume mesh has 430k nodes.

BOUNDARY CONDITIONS AND SIMULATION SETUP

As it is discussed in detail by Sick et al. [5], it is possible to get good estimation of the flow field behavior carrying out simulations on the draft tube alone, by imposing a steady, uniform and symmetric velocity profiles at the inlet. Like this, several works show a good correlation between experimental data and numerical results obtained from flow simulations on the draft tube without the runner. For this work, the geometry of the new runner was not taken into account as transient disturbances induced by passing runner blades were not the focus of the investigation; the main intention was to capture the global flow field through the draft tube.

The inlet boundary condition for these simulations are averaged steady velocity profiles of both circumferential and axial flow distribution at the exit plane of the runner, measured by using 2D LDV techniques in model tests. Radial velocity component is assumed negligible. Two off-design conditions are evaluated in order to investigate the draft tube flow behavior after optimization of other water passage ways; for both cases, averaged velocity profiles are shown in figures 3 and 4.

Case 1: H = 134.3 m, Q = 569.3 m^3/s

Case 2: H = 134.3 m, Q = 422.7 m^3/s

LDV measurements on model were taken at the position where the radius of the draft tube cone was 166.5 mm. To recalculate these velocity profiles at the inlet, the following relations are used: $rC_u = constante$ and continuity law for C_m. For all simulations a hydrostatic pressure gradient is established as outlet boundary condition equivalent to a tail water level of 126.5 m or submergence head of 10.5 m. A source term is also added to momentum equations as a pressure gradient scaled with the minimal local dynamic head. This term is defined by eqn. 8, where f should be an experimental value obtained from energetic studies on the physical model, however in this case, it was assumed $f = 3.3$.

$$\Delta P_{loss} = f \frac{C_n^2}{2} \tag{8}$$

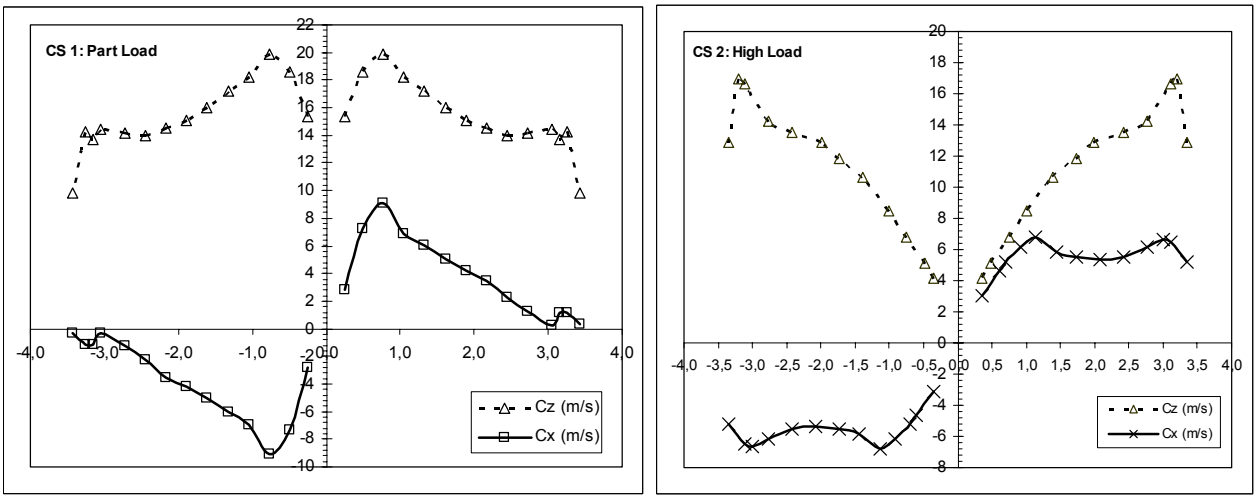

Figure 3: Circumferential and axial velocity distributions at the draft tube inlet for Case1 and Case2

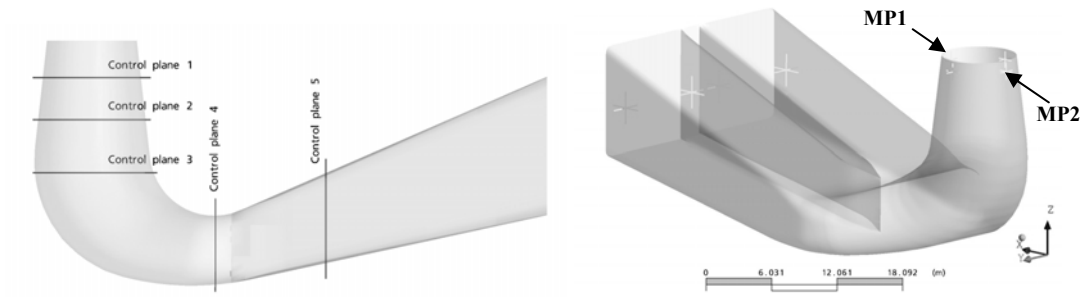

Figure 4: Control planes and monitor points for results visualization

Control planes are located on specific cross sections to visualize pressure and velocity profiles and also, monitor points are situated at the same place of pressure taps in the prototype, in order to estimate the pressure recovery factor appropriately.

PARTIAL LOAD UNSTEADY SIMULATION (Case 1)

The static pressure recovery factor (χ) is calculated using eqn. (4) in order to compare it with experimental data from prototype measurements. Then, the computed value is $\chi_{cal\_1} = 0.2619$, while the measured value is $\chi_{med\_1} = 0.292$. This difference is assumed to be originated by the very poor mesh quality on walls and therefore, the inability to capture boundary layer effects which have important influence on the prediction of draft tube efficiency.

$$\chi = (p_2 - p_1)/\rho C_1^2 \qquad (9)$$

For this case, an incoming swirling flow generates an asymmetric helical vortex structure from inlet down to the bend. The right channel is dominated by recirculation zones, because more than 70% flow is leaving through the left channel, basically for the topological evolution of the draft tube geometry. The development of the pressure field, at the same time, is shown at figure 6 (left side), where the vortex core reaches vapor pressure values and then, a cavitation region within the vortex rope is observed. It can be seen that an asymmetric and quasi-periodic pressure and force distribution between inlet and bend are cause of strong hydrodynamic instabilities.

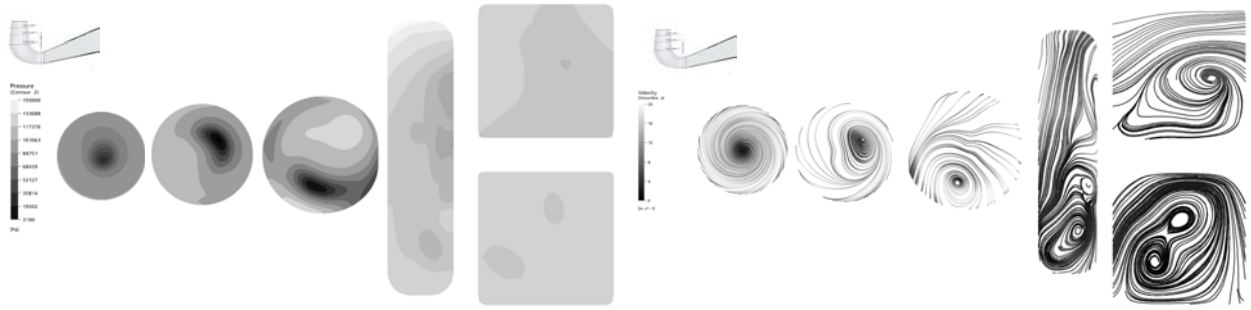

Figure 5: Pressure contours and planar velocity streamlines on control planes for Case1

Figure 5 (right side) shows velocity streamlines on control planes; it is noticeable a strong asymmetric behavior along each section in the draft tube and a rapid flow desacceleration after the bend. Subsequently, inside the right channel an intense curvature of streamlines indicates the formation of a vortex structure traveling along this channel. This vortex structure is more clearly observable on figure 6 (left) where the vortex core path is drawn in pointed red line, while on the right side; a constant pressure isosurface is plotted and compared with a photo of the physical phenomenon in model tests.

Figure 6: Velocity streamlines on control sections and vortex core pathway through a channel for Case1 (left). Constant pressure isosurface in comparison with a lab picture of vortex rope (right)

Unsteady behavior of vortex rope is studied by means of the evolution of hydrodynamic characteristics in time. All equations converged after more than 100 time-steps of 0.01s each one. Figure 7 shows constant pressure contours plotted every 0.2s on different control sections, where it

is possible to visualize the precession movement (rotational translation) of the vortex core in the rotation direction of the machine. These strongly pulsating pressure fields are clearly the main cause of very high pressure fluctuations for this specific operating condition.

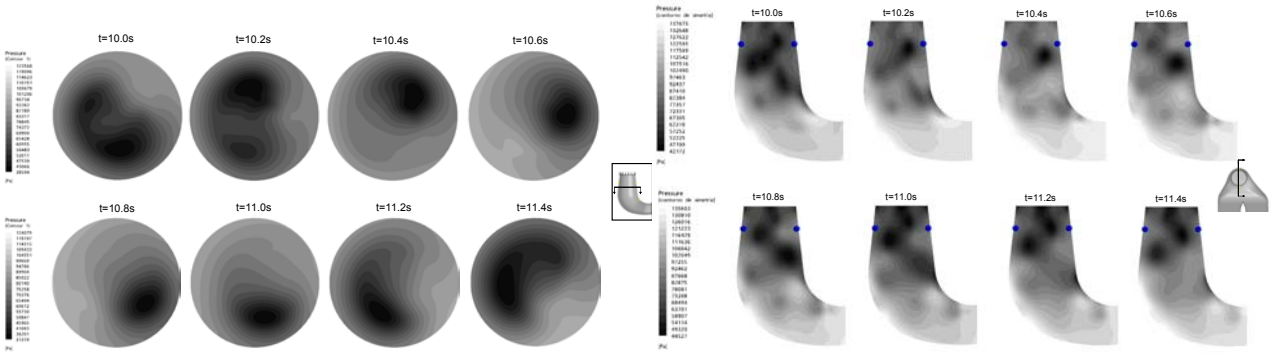

Figure 7: Transient behavior of pressure fields plotted on control sections for Case 1

In addition, to pressure and velocity contours, a constant pressure isosurface is used in order to capture the physical cavity volume changing while the vortex core is rotating. It is noticeable the poor resolution of volume due to the coarse mesh used, but it is enough to view the hydrodynamic effect of the flow on a cavitation vortex. Figure 8 shows a development of the cavity volume using a single phase model.

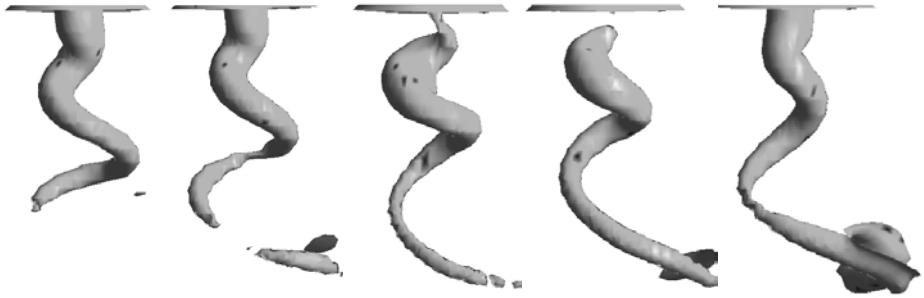

Figure 8: Change of position and volume of vortex rope for Case1

Computed and measured pressure fluctuations are compared in figure 9 in order to show the good agreement between them. In time domain, amplitudes are just about 16% underestimated; computed precession frequency response was 0.69 Hz in contrast to measured frequency of 0.6 Hz, demonstrating a slight frequency overestimated.

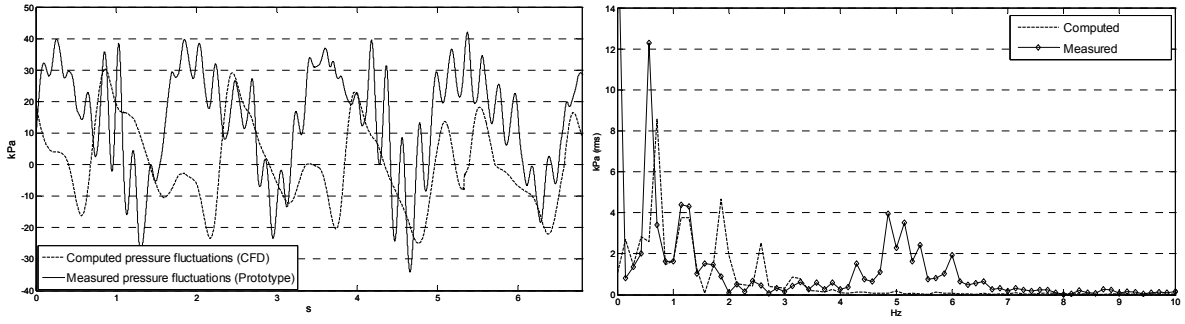

Figure 9: Pressure pulsations in time (left) and frequency domain (right), measured (blue) versus computed values (red)

In this way, it was captured the pressure fluctuations frequency response of the vortex rope at partial load using k-ε turbulent model and a relatively coarse mesh. These results are compared with

precedent investigations, and of course, compared against experimental data registered in the prototype. A quantitative summary is presented in the table 1.

Measurement Data Vs. Numerical Results	CFD $f_{vórtice}$/ Exp $f_{vórtice}$	CFD amplitud / Exp amplitud
Ruprecht et al. [k-ε]	0.93	0.7 – 1.3
Scherer et al.	1 (baja resolución)	1 – 1.4
Miyagawa et al.	No disponible	No disponible
Sick et al. [k-ε]	1.12	0.83
Ciocan et al. (FLINDT) [k-ε]	1.13	1
Arzola F. [k-ε]	0.87	0.84

Table 1: Quantitative comparison of numerical results versus experimental data

HIGH LOAD UNSTEADY SIMULATION (Case 2)

In this case study (Case 2), the static pressure recovery factor is also calculated in order to compare simulation with experimental data from prototype measurements. Thus, the computed value was $\chi_{cal\_2} = 0.2207$, while measured value was $\chi_{med\_2} = 0.287$. The coarse mesh and the reduced wall treatment are the main explanation for this rather awful prediction of draft tube performance. Moreover, it is evident a very low pressure recovery factor for both evaluated operating condition. Regarding to overall characteristics of flow field at high load, the inlet velocity profiles induced a more uniform flow along the water passage, including channels. Figure 10 shows pressure and velocity distributions over transversal control planes where it is observable the concentricity of the vortex core and how streamlines rotate as the radius toward the axis line diminishes.

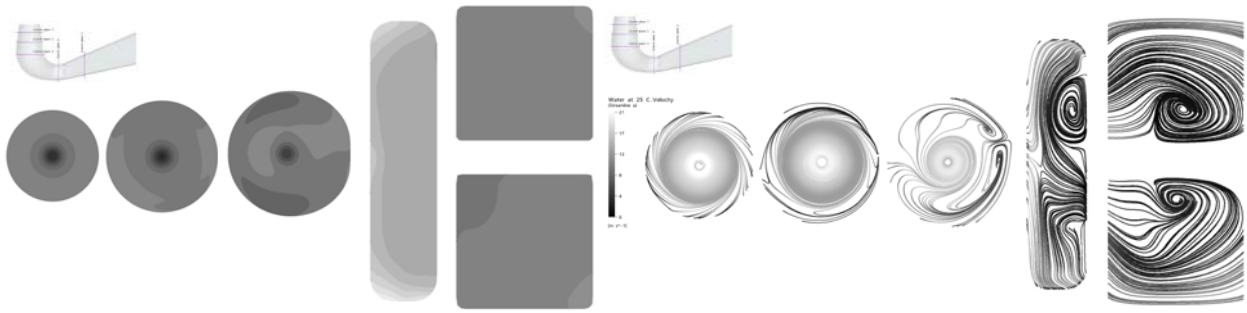

Figure 10: Pressure contours and planar velocity streamlines on control planes for Case 2

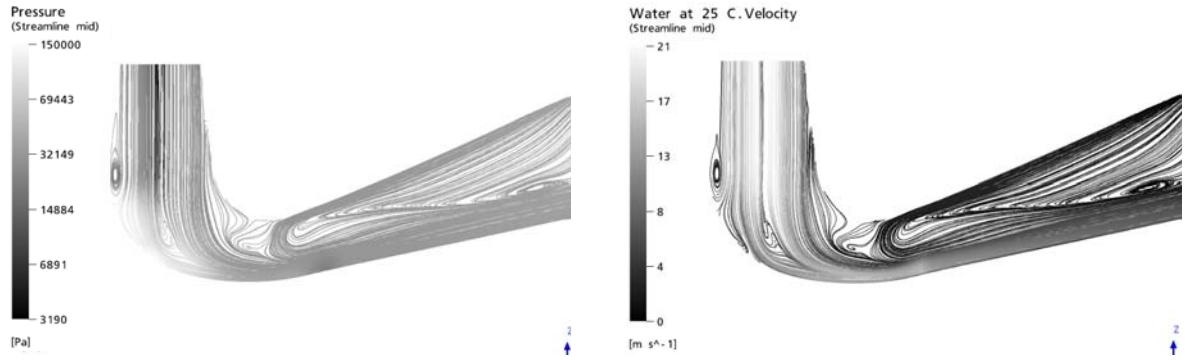

Figure 11: Pressure and velocity streamlines on transversal control plane for Case 2

As it can be seen in figure 11, an axisymmetric vortex attached to the runner cone travels downstream and hits directly the bend floor and consequently causes a great flow separation on both channels. Separation zones are clearly located on cone, bend and channels and it is quite

evident that most of the water flow is being evacuated through the lower sides of both channels. The flow field leads to the formation of two big vortices, one along each channel until arriving to the exit, as it is shows in figure 12.

Figure 12: Vortex pathways and velocity streamlines on control planes for Case 2

It is studied the evolution in the time of the pressure field which is characteristic of the fluctuating hydrodynamic parameters. The time-dependant flow behavior for this condition is far away to be captured using these basic simulation parameters. After a lot of converged time steps, there are still not obvious changes on volume and shape of the constant pressure isosurface and therefore, there are not pressure fluctuations amplitudes captured in the simulation, as it is shown in figure 13.

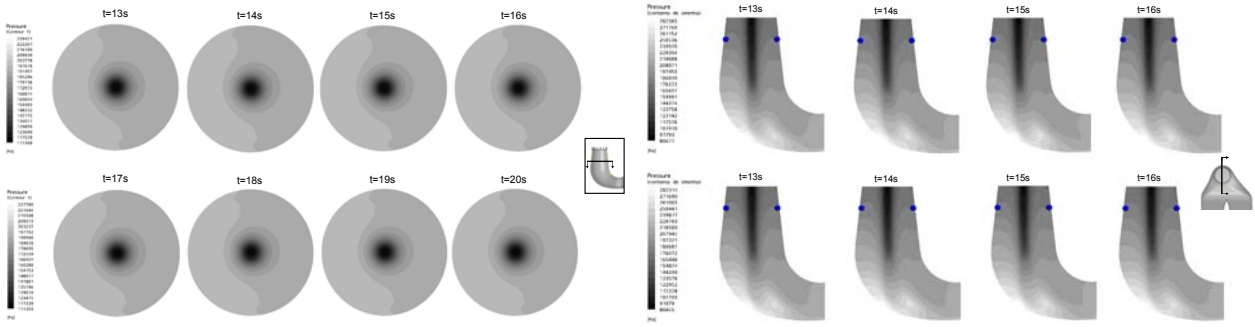

Figure 13: Pressure distribution contours on control sections for Case 2

CONCLUDING REMARKS

It is necessary to highlight the fact, that although it is not trivial to reproduce unsteady conditions from steady initial conditions and permanent - symmetrical boundary conditions, it was possible to solve the unsteady complex rotating vortex flow, starting from steady and symmetrical boundary conditions, without needing to simulate the runner coupled to the draft tube.

Self-excited instabilities, recirculation and cavitation regions still appears in off-design operating conditions, even though after overhaul a better global performance was reached successfully with a hydraulically optimized runner.

The implemented methodology was useful to reach a good agreement in the partial load simulations (Case 1), but for high loads (Case2) it was not possible to obtain the experimentally observed hydrodynamic parameters. To numerically simulate free oscillations in the draft tube or draft tube void, it is necessary to implement a two-phase model that takes into account the vapor compressibility (cavitation compliance) and the mass transfer among phases.

For industrial purposes, it is possible to simulate the global hydrodynamic behavior of hydraulic turbines with limited computational resources in order to understand the complexity of unsteady phenomena that happen while the machine operates inside or outside of its operating range.

BIBLIOGRAPHICAL REFERENCES

[1] PRENAT J-E. (2000). *Instability in hydraulic machines. Specific problems for Francis turbines.* Inter-university specialized course IMHEF-EPFL & INPG. Switzerland.

[2] MAURI S (2002). *Numerical Simulation and Flow Analysis o fan Elbow Diffuser*. Ph.D. Thesis No. 2527, EPFL. Switzerland.

[3] ARZOLA F, MARQUEZ A (2004): *A technical assessment of improvements on large refurbished turbines at Guri Hydroelectric Complex*. Proceedings of 22nd IAHR Symposium on Hydraulic Machinery and Systems, Vol. A, A13-1. Sweden, Stockholm.

[4] STEIN P, SICK M, DOERFLER P, WHITE P, BRAUNE A (2006). *Numerical Simulation of a cavitating draft tube vortex in a Francis turbine.* Proceedings of 23rd Symposium on Hydraulic Machinery and Systems. Yokohama, Japan.

[5] SICK M, DOFLER P, SALLABERGER M, LOHMBERG A, CASET M (2002). *Simulation of the Draft Tube Vortex.* Proceedings of 21st Symposium on Hydraulic Machinery and Systems. Switzerland, Lausanne.